JOURNAL OF MATERIALS SCIENCE 37 (2002) 813–818

Joining of ZrO_2-4.5 wt% Y_2O_3 (Y-TZP) ceramics using nanocrystalline tape cast interlayers

B. G. RAVI*, R. CHAIM
Department of Materials Engineering, Technion - Israel Institute of Technology, Haifa 32000 Israel
E-mail: rchaim@tx.technion.ac.il

Nanocrystalline Y-TZP tape casts were used as interlayers to join conventional Y-TZP ceramic pellets. The joining experiments were performed by hot pressing at 1000°C to 1300°C under constant pressure of 55 MPa. Two types of joints were obtained with and without a nanocrystalline interlayer. At 1100°C, the successful joints were enabled only with the interlayer; four point bending test results revealed an average joint strength of 206 ± 10 MPa. The joint strength increased with the joining temperature. The specimens joined at 1300°C with an interlayer exhibited a joint strength of 613 ± 40 MPa, which is ~96% of the strength of the ceramic pellets. The interlayer at the joint exhibited homogeneous and crack free microstructure and preserved its nanocrystalline nature at all temperatures. The advantage of the nanocrystalline interlayer for joining is pronounced at lower joining temperatures and most probably for pellets with large grain size.

1. Introduction

Recent developments in production of nanocrystalline yttria stabilized tetragonal zirconia polycrystal (Y-TZP) powders has led to the fabrication of dense ultrafine grained ceramics, exhibiting superplastic behavior above 1100°C [1, 2]. Advantage was taken of this enhanced superplasticity to join nanocrystalline Y-TZP pellets to themselves [3], between submicron Y-TZP's [4–6], zirconia multilayers [7] and to alumina [8]. However, joining of conventional zirconia ceramics that do not plastically deform at these temperatures necessitates the use of ultrafine grained interlayers which deform superplastically and interlock the surface grains. Presintered as well as slurry interlayers of nanocrystalline and submicron sized Y-TZP were used to join commercial Y-TZP [9] and alumina ceramics [10]. Successful joints were made between Y-TZPs using the presintered (90% dense) nanocrystalline (180 nm) interlayers at 1090°C for 5 h under the uniaxial pressure of 10 MPa [9]. However, in all these cases, porosity was present at the joint interfaces, either due to the large shrinkage of the nanocrystalline interlayer, or due to the thermal expansion mismatch between the alumina and zirconia. In addition, no data is available on the mechanical properties of such joints. Recently, successful joining of alumina pellets using nanocrystalline alumina tape cast interlayers was demonstrated [11].

The present paper describes the fabrication, microstructure and mechanical properties of the joints made between conventional yttria stabilized tetragonal zirconia polycrystal (Y-TZP) pellets using nanocrystalline Y-TZP tape cast interlayers.

2. Experimental procedure

Fully dense cylinders of 20 mm in length and 15 mm in diameter were prepared by cold pressing (at 200 MPa) and pressureless sintering of a commercial Y-TZP powder (HSY-3) at 1450°C for 10 h. The bonding surfaces, perpendicular to the cylinder axis, were polished using 600 grit SiC abrasive paper. Finally, the substrates were cleaned in the ultrasonic bath using ethanol and then acetone. Commercial nanocrystalline Y-TZP powder (Tioxide; 75 nm average particle size) was used to form the tape casts. The non-aqueous formulation of the best tape casts was (in gr): 100 powder, 28 Xylene, 28 Ethyl Alcohol, 6 Dibutyl Pthalate, 6 Polyethylene glycol, 5 Polyvinyl butyral, and 2.4 Menhaden Fish oil. This formulation enabled flexible and deformable tape casts which could be manually handled at thicknesses lower than 100 μm.

The set-up of the tape cast interlayer, sandwiched between two cylinders, was uniaxially cold pressed under the load of 2 KN, followed by hot pressing at high temperatures. Two loading regimes were applied:

2.1. Regime (a) : Dead load joining

The preliminary tests were performed at different temperatures and durations, using a 0.5 Kg dead load (43 KPa) within a regular furnace. The aim of these tests

Present Address: Materials Modification Inc. 2721-D, Merrilee Drive, Fairfax, Virginia 22031 USA.

TABLE I Dead load joining of Y-TZP specimens using nano Y-TZP interlayer

Sample #	Temperature [°C]	Duration [h]	Remarks
1	1100	5	No bond
2	1100	10	No bond
3	1150	5	Weak/defective bond
4	1150	10	Good/defective bond
5	1200	10	Successful bond
6	1250	10	Successful bond
7	1300	10	Successful bond

were to determine whether bonding is possible under a relatively low static pressure. The joining conditions and results were summarized in Table I.

2.2. Regime (b) : Quasi-static load joining

Two types of joining experiments were performed in regime (b), that is joining *with* and *without* a tape cast interlayer the experimental conditions are summarized in Table II. Load was applied at room temperature to the sandwich set-up until the tape flow outside the joining area, to ensure the tape held firmly in between the pellets. This preloading (8.6 MPa) was kept constant while the temperature was increased (at the rate of 5°C/min) to the actual joining temperature. Then, the load was increased to the desired stress level (55 MPa). The joining duration was considered from the time at which the load reached the desired level. The length and diameter of the cylinders and the set-up were measured prior to and after the joining in order to calculate the plastic strain during the joining process.

The resultant cylinders were cut along their axis to four bar-shaped specimens, with dimensions of $3 \times 3.5 \times 24$ mm for bending tests. The bars were polished with 600 grit SiC abrasive paper along their length, and their edges were chamfered at 45°. The 4-point bending tests were performed using a cross head speed of 0.1 mm/min in an Instron machine; the outer and inner spans were 20 and 10 mm, respectively. The joint area as well as the fracture surfaces in bending were gold evaporated and characterized using scanning electron microscopy (SEM).

3. Results and discussion

3.1. Fabrication and mechanical properties

The bonding conditions were selected step by step with respect to the results of the preceding experiments. Visual inspection for the joint quality of the specimens in the regime (a) (shown in Table I under 'Remarks') indicated that joining is possible at low stresses and low temperatures (1150°C). It also indicated that the selected temperature range was appropriate for the further joining experiments. Nevertheless, these conditions neccessitated long joining durations, with inevitable residual porosity both at the pellet/interlayer interfaces and within the nanocrystalline interlayer (Fig. 1). Thus, regime (b) was adopted for the detailed joining studies. In this regime, the pressure level and the joining duration were kept constant (55 MPa and 1 h, respectively), and the temperature was increased in steps of 100°C as summarized in Table II. Few joining experiments were also performed for longer durations in order to study the bond quality with respect to time. The bending strength as well as its average values are also presented in Table II. In bending tests, the fracture occured in all the specimens at the joint interfaces (except for 1300°C/1h/55 MPa without interlayer).

No joining took place at 1000°C regardless of the presence or absence of the nanocrystalline interlayer, as indicated in Table II. However, successful joint was formed at 1100°C only with the use of the interlayer. At this temperature, the plastic deformation of the pellets was negligible and unmeasurable. The average bending strength of these joints was relatively high (206 MPa) with a very low standard deviation (±10 MPa). This low standard deviation is a clear indication of the very homogeneous nature of the joint. This joint strength is estimated to be more than 30% of the bending strength of the sintered pellets (see further discussion below). Increasing the bonding duration to 5 h at 1100°C, resulted in an improved joint strength (i.e. maximum strength of 240 MPa compared to 216 MPa) eventhough the average bending strength was not changed (206 versus 204 MPa).

Further increase of the joining temperature to 1200°C rendered successful joints in the specimens where no nanocrystalline interlayer was present. However, at this temperature, both types of specimens exhibited 2%

TABLE II Characteristics of the joining experiments at 55 MPa

Temperature [°C]	Duration [h]	Remarks (% strain)	Bending strength [MPa]	Average strength [MPa]
With interlayer				
1000	1	No bond	- - - - - - -	- - - - - - -
1100	1	Bonded (0%)	196; 207; 216	206 ± 10
1100	5	Bonded	137; 201; 236; 241	204 ± 48
1200	1	Bonded (2%)	234; 249; 253; 260	249 ± 11
1300	1	Bonded (15%)	558; 615; 630; 650	613 ± 40
No interlayer				
1000	1	No bond	- - - - - - -	- - - - - - -
1100	1	No bond	- - - - - - -	- - - - - - -
1100	5	No bond	- - - - - - -	- - - - - - -
1200	1	Bonded (2%)	236; 344	290 ± 76
1300	1	Bonded (15%)[a]	538; 628; 749	638 ± 106

[a]Fracture occured outside the joining interface, in contrast to fracture at the joining interface in the other specimens.

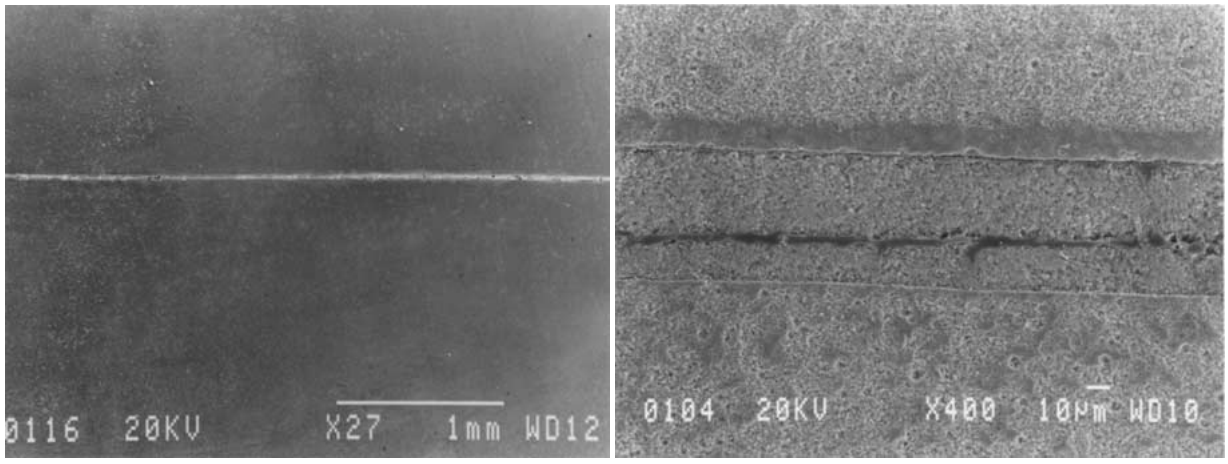

(a) (b)

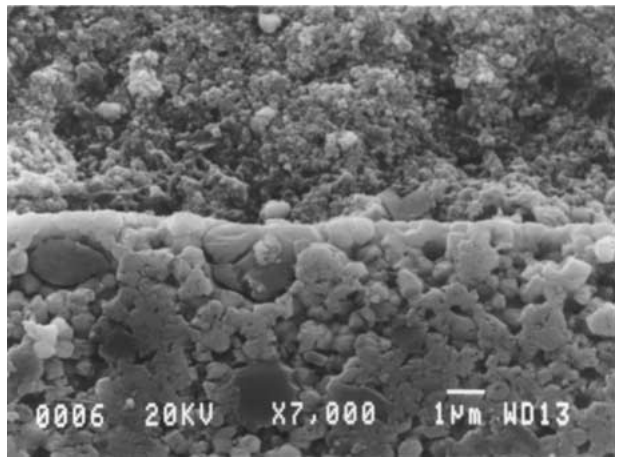

(c)

Figure 1 SEM images of the Y-TZP joints formed with nanocrystalline interlayer under small static load (regime A) at 1200°C/10 h. (a) Low magnification. (b) Higher magnification (c) Grain size in the interlayer (nanometric) and the pellet (submicron).

compressive strain along the cylinder length. The specimens having the interlayer exhibited similar degree of joint homogeneity as in the previous joints. This was indicated by the low standard deviation of the bending strength (±11 MPa). Nevertheless, as expected, higher values of bending strength of joints were measured (250 MPa in average) for this specimen. On the other hand, specimens without the interlayer also exhibited higher strengths in an average of 290 MPa. However, only two specimens were available exhibiting the bending strength of 236 MPa and 344 MPa. Although the large difference between these two results has no statistical importance, it reveals the less homogeneous nature of the joint compared to its counterpart specimen, that with the interlayer.

Further increase in the joining temperature to 1300°C led to a significant plastic deformation (15%) in both types of specimens. The average bending strength in

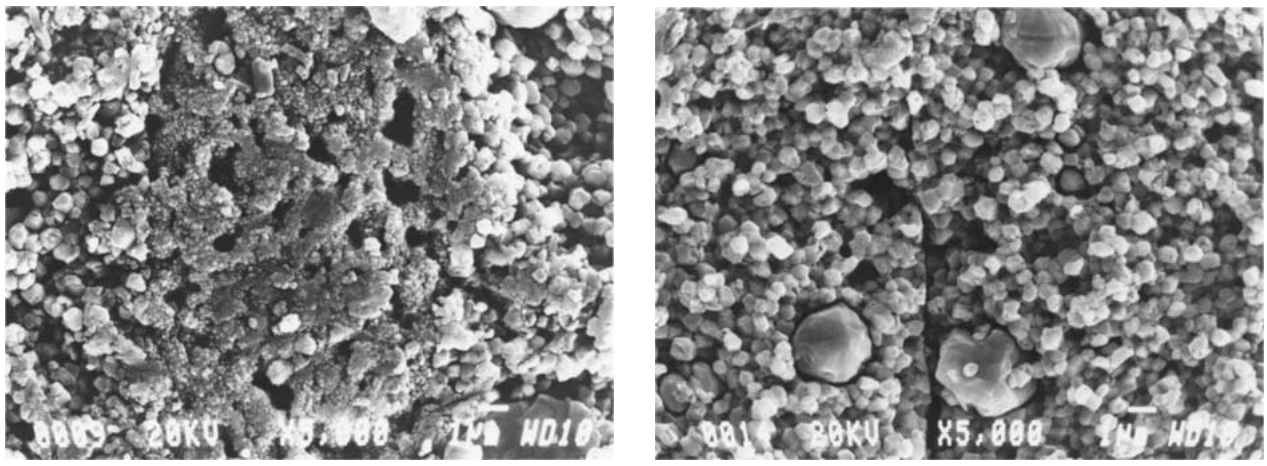

(a) (b)

Figure 2 SEM images of the joints formed by hot-pressing at 1200°C/55 MPa/1 h (a) with and (b) without the nanocrystalline interlayer.

the specimens with the interlayer increased to 613 MPa, about 96% of the strength of the pellets. These specimens fractured at the joint interface. For comparison, the counterpart specimens, without the interlayer, fractured outside the original joint interface. Thus, the bending strength in these latter specimens was considered to represent the strength of the pellets (with an average strength of 638 MPa). The fact that all the specimens, except this series, were fractured at the joint interfaces indicates that the measured bending strength represent the actual strength of the joints.

On the other hand, relatively high standard deviations were observed in the strength of the specimens without the interlayer compared to those with it. This may point

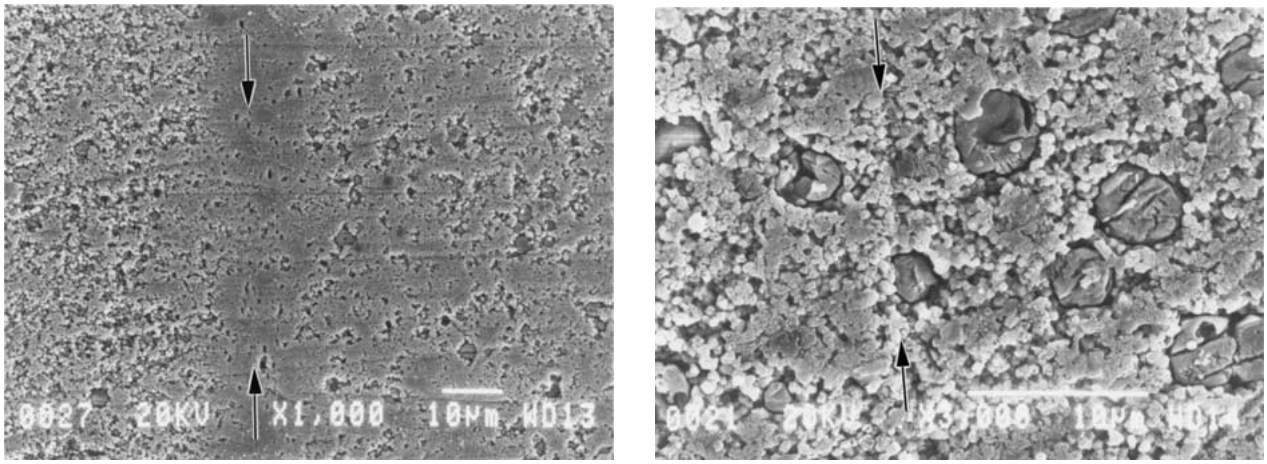

(a) (b)

Figure 3 SEM images of the joints formed by hot-pressing at 1300°C/55 MPa/1 h (a) with and (b) without the nanocrystalline interlayer. The original joint interfaces were indicated by arrows.

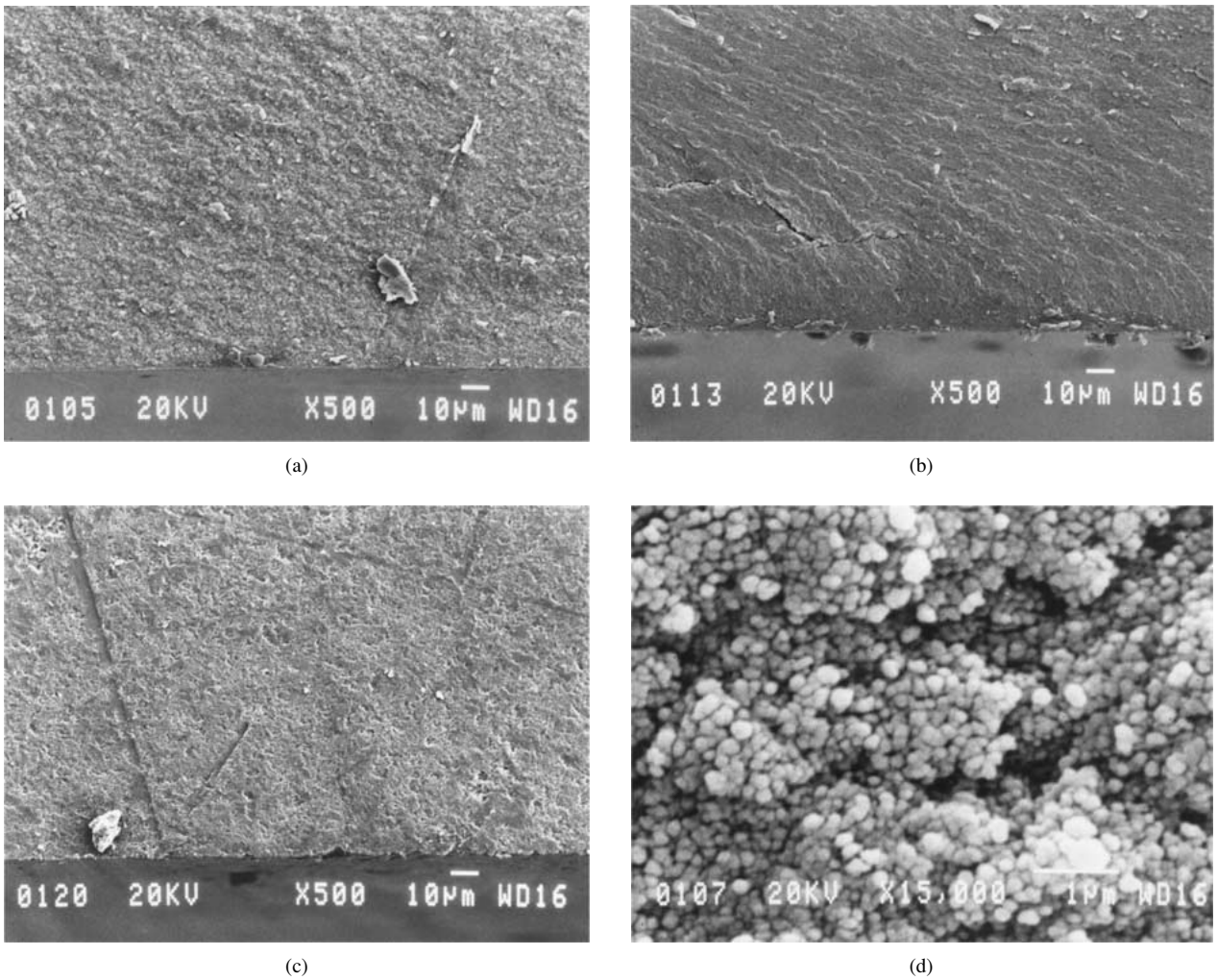

(a) (b)

(c) (d)

Figure 4 Fracture surfaces near the face under tensile. Joints with the nanocrystalline interlayer formed under 55 MPa at (a) 1100°C and (b) 1200°C, and without the interlayer at (c) 1200°C, showing relatively smooth fracture surfaces. Traces of the polishing lines are visible in (c). (d) Higher magnification from (b) reveals the nanocrystalline nature of the interlayer.

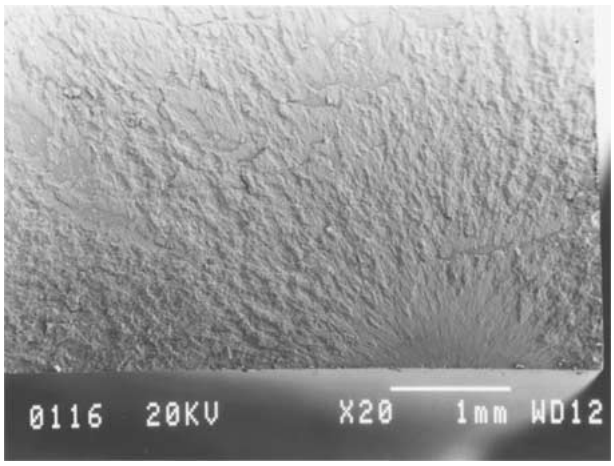

(a)

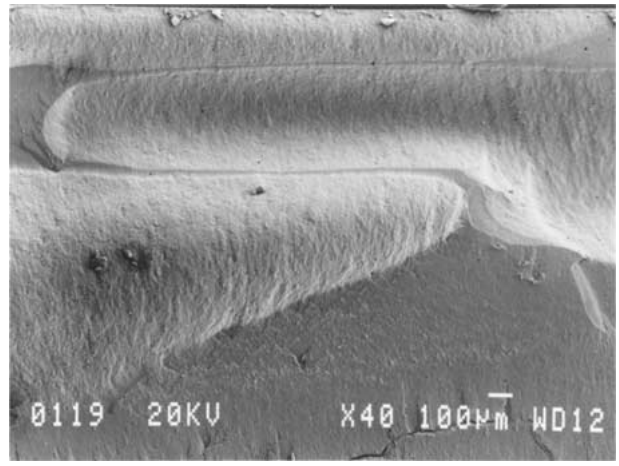

(b)

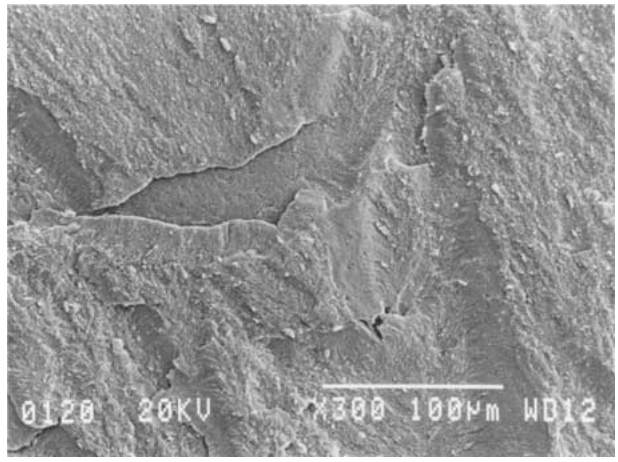

(c)

Figure 5 Fracture surfaces from the joints with the nanocrystalline interlayer formed under 55 MPa at 1300°C. (a) The crack origin, mirror and hackle are visible near the face originally under tensile. (b) Strong crack deflection and bumps near the face originally under compression. (c) Crack deflection and branching leading to the 'river pattern' on the fracture surfaces.

to a more homogeneous distribution of the defects at the joint in the latter specimens.

3.2. Microstructure and fractography

Typical SEM images exhibiting the joint microstructure in regime (a) are shown in Fig. 1. Low magnification images (i.e. Fig. 1a) showed the presence of voids and discontinuities at the joints, eventhough good joints were formed. Nevertheless, part of the voids were formed during cutting and polishing for preparation of SEM specimens. Thermal etching also was found to introduce cracks at the joining interfaces indicating the existence of very weak bonds at these interfaces. At these joining conditions, the originally $\sim$100 μm thick interlayer tape densified and shrank to the thickness of 40 to 60 μm (Fig. 1b). At higher magnifications, porosity is evidenced in the nanocrystalline interlayer, in comparison to the adjucent pellets (Fig. 1b). Nevertheless, the same type of specimen, after fine polishing and chemical etching, exhibited a continuous joint interlayer (Fig. 1c); the nanocrystalline nature of the interlayer was preserved. Since thermal etching was found to damage the joint interface, the specimens were etched chemically for SEM analysis.

The microstructure of the joints formed in regime (b) at 1200°C for 1 h with and without the interlayer, are shown in Fig. 2a and b, respectively. At low magnifications (not shown here) a few voids were observed at the interlayer/pellet interfaces. At higher magnifications, both types of specimens exhibited excellent continuity along the joint area. The specimens without the interlayer, revealed crack-like defects (Fig. 2b) that resemble the non-bonded areas at the joint interfaces. In the counterpart specimens, the interlayer was distinguished from its adjucent pellets only due to their distinct grain size (Fig. 2a).

Joints made at higher temperatures (i.e. 1300°C) using the interlayer, were almost defect-free (Fig. 3a). One to two void-shape defects, 2 to 10 μm in length were observed along the entire width (3.5 mm) of the specimen. In the specimens without the interlayer (Fig. 3b), the joining interface cannot be distinguished except at a few locations (where contrast resembling the original interface was present, as arrowed in Fig. 3b). The last two types of specimens exhibited similar joint strength.

Fracture surfaces of the joints made at 1100°C and 1200°C with and without the interlayer are shown in Fig. 4a–c. The fracture surface was smooth in all specimens, and located at the original joint interface. Some

delamination as well as microcracking were observed in the interlayer joined at 1200°C (Fig. 4b). The latter fracture surface at higher magnifications (Fig. 4d) revealed a nanocrystalline nature, indicating that the crack has been propagated through the joint interlayer. On the other hand, traces of the unannealed polishing grooves were found on the fracture surfaces of the counterpart specimen, that without the interlayer (Fig. 4c). This might be an indication of partial bonding at these interfaces. In contrast, the presence of the interlayer enabled the formation of chemical bonds at the joint interfaces, most probably due to both the rapid sintering and the densification by superplastic deformation [1, 7, 9, 12] of the nanocrystalline interlayer grains at the joint interface.

The important microstructural feature that differentiated between the joints with the interlayer formed at 1100°C–1200°C (Fig. 4a and b) and 1300°C (Fig. 5) was the fracture morphology near the surfaces originally subjected to the tensile and compressive stresses. The high strength joints, formed at 1300°C, were characterized by relatively rough fracture surfaces. The fracture surface at the tensile side often contained a crack source followed by the typical mirror, mist and hackle (Fig. 5a). The fracture surface at the compressive side was often characterized by strong crack branching and bumps near the face of the specimen (Fig. 5b). In addition, careful observation of the fracture surfaces revealed morphologies similar to that of the 'river pattern' (Fig. 5c). As was shown above, the low strength joints, formed at lower temperatures, exhibited relatively smooth fracture surfaces and lacked these morphological details. The latter details often characterize fracture surfaces of glasses or ceramic single crystals [13]. Development of these morphological details in dense and homogeneous materials depends on the crack velocity and the strain energy release rate, as well as on the intrinsic flow size. As the strain energy release rate increases due to the higher joint strength, the transition between the quasi-static crack propagation to the dynamic condition is accelerated. This transition gives rise to crack acceleration already at the mirror region, followed by crack deflections and branching in the dynamic conditions (i.e. hackle and the 'river pattern'). Decrease in the flow size has a similar effect in accelerating the transition to the dynamical crack growth. Thus the relatively smooth fracture surfaces in the low strength joints are associated with very slow crack propagation as well as large flow sizes, in agreement with the microstructural observations. Consequently, the presence of these morphological details is indicative of dense, high strength and defect-free joints.

Finally, it is apparent that at temperatures above 1200°C, no advantage remains for the interlayer as a joining medium. This is due to the submicron grain size of the pellets which undergo plastic deformation at these temperatures [12, 14]. Therefore, the use of nanocrystalline interlayer may be advantageous even at higher joining temperatures for pellets with larger grain size.

4. Summary and conclusions

Nanocrystalline Y-TZP powders were used as tape cast interlayer for joining of conventional Y-TZP ceramics by hot-pressing. Joining experiments were performed both with and without a nanocrystalline interlayer, and at different joining conditions (temperature/pressure/duration). From the mechanical test results in bending and microstructural characterization of the joints and their fractography, the following conclusions can be drawn:

1. Joining of coventional Y-TZP by the aid of nanocrystalline Y-TZP tape cast interlayer was enabled by hot-pressing at temperatures as low as 1100°C for 1 h duration, where no joining was possible without the interlayer at these conditions.
2. Increase in the joint bending strength was associated with increase of the joining temperature and duration.
3. The advantage of the nanocrystalline interlayer for joining is pronounced at lower joining temperatures and most probably for pellets with large grain size.

Acknowledgments

The authors thank the Israel Ministry of Science, Culture and Sports for supporting this research through the infrastructure grant # 5878-2-96. Dr. Dov Sherman is acknowledged for performing the bending tests and helpful discussions.

References

1. L. CHEN, T. ROUXEL, R. CHAIM, H. VESTEGHEM and D. SHERMAN, *Mater. Sci. Forum* **243–245** (1997) 245.
2. F. GUTIERREZ-MORA, A. DOMINGUEZ-RODRIGUEZ, M. JIMENEZ-MELENDO, R. CHAIM and M. HEFETZ, *NanoStructured Materials* **11** (1999) 531.
3. M. J. MAYO, *Materials & Design* **14** (1993) 323.
4. J. YE and A. A. DOMINGUEZ-RODRIGUEZ, *Scripta Metall. Mater.* **33** (1995) 441.
5. A. A. DOMINGUEZ-RODRIGUEZ, E. JIMENEZ-PIQUE and M. JIMENEZ-MELENDO, *Scripta Mater.* **39** (1998) 21.
6. T. H. CROSS and M. J. MAYO, *NanoStructured Mater.* **3** (1993) 163.
7. A. A. DOMINGUEZ-RODRIGUEZ, F. GUIBERTEAU and M. JIMENEZ-MELENDO, *J. Mater. Res.* **13** (1998) 1631.
8. T. NAGANO, H. KATO and F. WAKAI, *J. Amer. Ceram. Soc.* **73** (1990) 3476.
9. F. GUTIERREZ-MORA, A. A. DOMINGUEZ-RODRIGUEZ, J. L. ROUTBORT, R. CHAIM and F. GUIBERTEAU, *Scripta Mater.* **41** (1999) 455.
10. Y. MOTOHASHI, T. SAKUMA and C. C. CHOU, in THERMEC'97, Inter. Conf. On Thermomechanical Processing of Steels & Other Materials, 1997, edited T. Chandra and T. Sakai (The Minerals, Metals & Materials Society) p. 1999.
11. R. CHAIM and B. G. RAVI, *J. Mater. Res.* **15** (2000) 1724.
12. M. JIMENEZ-MELENDO, A. DOMINGUEZ-RODRIGUEZ and A. BRAVO-LEON, *J. Amer. Ceram. Soc.* **81** (1998) 2761.
13. R. W. RICE, in "Advances in Ceramics," Vol. 22, Fractography of Glasses and Ceramics, edited by J. R. Varner and V. D. Frechette (Am. Ceram. Soc. Inc., Ohio, 1988) p. 3.
14. D. M. OWEN and A. H. CHOKSHI, *Acta Mater.* **46** (1998) 667.

Received 21 September 2000
and accepted 4 October 2001